Two degrees of freedom parallel linkageto track solarthermal platforms installed on ships

I Visa[1], A Cotorcea[1, 2] M Moldovan[1] and M Neagoe[1]

[1]Renewable Energy Systems and Recycling Research Centre, Transilvania University of Brasov, Romania
[2]Department of Naval and Port Engineering and Management, MirceacelBatran Naval Academy, Romania

E-mail: visaion@unitbv.ro

Abstract. Transportation is responsible at global level for one third of the total energy consumption. Solutions to reduce conventional fuel consumption are under research, to improve the systems' efficiency and to replace the current fossil fuels. There already are several applications, usually onsmall maritime vehicles, using photovoltaic systems to cover the electric energy demand on-board andto support the owners' commitment towards sustainability. In most cases, these systems are fixed, parallely aligned with the deck; thus, the amount of solar energy received is heavily reduced (down to 50%) as compared to the available irradiance. Large scale, feasible applications require to maximize the energy output of the solar convertors implemented on ships; using solar tracking systems is an obvious path, allowing a gain up to 35...40% in the output energy, as compared to fixed systems. Spatial limitations, continuous movement of the ship and harsh navigation condition are the main barriers in implementation. This paper proposes a solar tracking system with two degrees of freedom, for a solar thermal platform, based on a parallel linkage with sphericaljoints, considered as Multibody System. The analytical model for mobile platform position, pressure angles and a numerical example are given in the paper.

1. Introduction

Solar tracking systems functionality consists of changing the platform'sposition (supporting solar thermal collectors or photovoltaic modules) to follow the apparent path of the Sun on the sky and thus to increase the amount of input solar radiation and, consequently, the output energy up to 35% comparing to fixed, optimally tilted, systems [1, 2]. The Sun-Earth geometry is described through a pair of angles: solar elevation angle (α) and solar azimuth angle (ψ) as in figure 1.

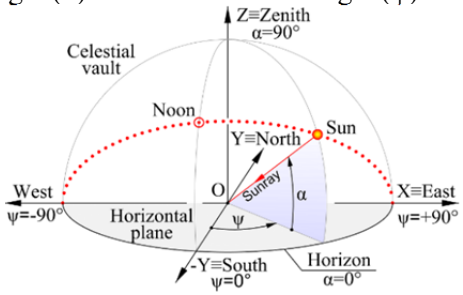

Figure 1. Solar elevation angle (α) and solar azimuth angle (ψ) describing Sun-Earth geometry.

For ground mounted solar tracking systems, these values range between 0° and 90° for the elevation angle and usually between 0° and 240° for the azimuth angle depending on the day and implementation location [3]. Usually, these motions can be done using serial and parallel mechanisms [1, 4].

According to figure 1, these angles are described in the OXYZ system corresponding to the local horizontal plane, where the OX axis has the East-West direction and positive sense toward to the East, the OY axis has the South-North direction and positive sense toward North, and OZ axis perpendicular to the local horizontal plane with upward positive sense for right orthogonal OXYZ system.

The tracking mechanisms for the platforms installed in a concrete and fixed location have the mobility M=2, usually by two successive rotations around two well defined axes, from which one is a fixed axis and the second one is a mobile axis. The diversity of these tracking mechanisms and the required rotation angles of theplatform were previously described [1] for all types of tracking mechanisms: azimuthal, pseudo-azimuthal, pseudo-equatorial and equatorial. For all these systems, the rotation angle around the fixed axis is an absolute angle and the rotation angle around the mobile axis is a relative angle. In this case, for each independent rotation a specific mechanism is used (linkage type, gears type, cam type etc.), using as independent driving motions translation (linear actuator) or rotation (rotary actuator). Very often linear actuators are used. A complex solution of this type, based on a four bar mechanism is described in [5] and is sketched in figure 2a.

The tracking mechanisms based only on absolute angles (directly related to the basis) are of parallel linkage type. In this case, both drivers are connected between the basis and the tracked platform. Literature mentions these types of tracking parallel linkages having mobility M=2, as in figures 2b [6], 2c [7] and 2d [8].

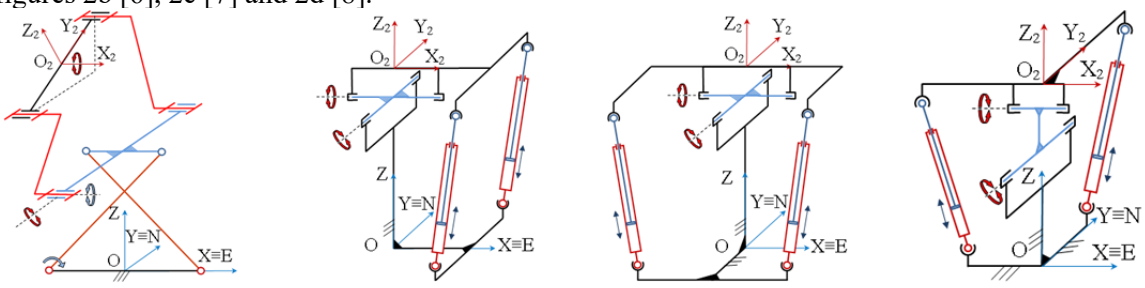

(a) (b) (c) (d)

Figure 2. Tracking mechanisms of parallel linkages type with M=2.

For a fixed location, all the previously described mechanisms allow the necessary motions by an optimal design. Solar tracking systems installed on the ships, i.e. with a changing location, must meet additionally requirements defined by the ship motion on different directions and latitudes, and by roll and pitch motions. In this case, the tilt angle and diurnal tracking motion cover a much broader range, and as a result new tracking mechanisms must be considered.

This paper investigates a new type of parallel linkage, with mobility M=2, based on spherical joints and driving linear actuators, to be used as tracking mechanism feasible for solar tracking systems on the ships.

(a) (b)

Figure 3. Proposed parallel tracking mechanism with M=2: CAD model (a) and structural scheme (b).

2. MBS structure of the parallel tracking linkage

The general form of the mechanism (in figure 3) consists of: the basis (1), the mobile platform (2), four sphere-sphere (SS) connections between the two bodies, and two linear actuators connected between the bodies, according to structural synthesis described in [6] by using Multibody System Method (MBS) [9]. The characteristics of the kinematical constraints are presented in table 1.

Table 1. The characteristics of the kinematic constraints between bodies.

Location	**Type**	**Bodies**	**Kinematic constraints c_{ij}**
AA_2	SS	1-2	1
BB_2	SS	1-2	1
CC_2	SS	1-2	1
DD_2	SS	1-2	1
Sum of kinematic constraints $\Sigma c_{ij} = 4$			

The mechanism mobility (M) is calculated using equation (1), for a number of two bodies ($n_b = 2$) in the general space (S = 6), having the sum of kinematic constraints $\Sigma c_{ij} = 4$:

$$M = S \cdot (n_b - 1) - \Sigma c_{ij} = 6 \cdot (2 - 1) - 4 = 2 \quad (1)$$

The mechanism mobility is equal with the number of the driving constraints represented by the two linear actuators $PP_2$and QQ_2, in figure 3b.

3. The parallel tracking linkage geometry

To define the geometrical model, two reference systems are used: the system OXYZ of the local horizontal plane of the body 1 and the system $O_2X_2Y_2Z_2$ of the mobile platform 2.

Table 2. Geometrical model of the bodies.

Body	**Scheme**	**Cartesian coordinates**
Body 1	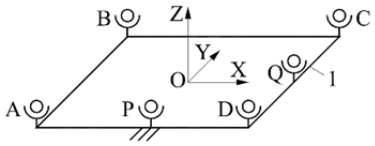	$[A] = \begin{bmatrix} X_A \\ Y_A \\ Z_A \end{bmatrix}$, $[B] = \begin{bmatrix} X_B \\ Y_B \\ Z_B \end{bmatrix}$, $[C] = \begin{bmatrix} X_C \\ Y_C \\ Z_C \end{bmatrix}$ $[D] = \begin{bmatrix} X_D \\ Y_D \\ Z_D \end{bmatrix}$, $[P] = \begin{bmatrix} X_P \\ Y_P \\ Z_P \end{bmatrix}$, $Q = \begin{bmatrix} X_Q \\ Y_Q \\ Z_Q \end{bmatrix}$
Body 2	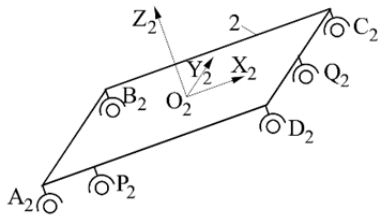	$\left[A_2^{(2)}\right] = \begin{bmatrix} X_{A_2}^{(2)} \\ Y_{A_2}^{(2)} \\ Z_{A_2}^{(2)} \end{bmatrix}, \left[B_2^{(2)}\right] = \begin{bmatrix} X_{B_2}^{(2)} \\ Y_{B_2}^{(2)} \\ Z_{B_2}^{(2)} \end{bmatrix}, \left[C_2^{(2)}\right] = \begin{bmatrix} X_{C_2}^{(2)} \\ Y_{C_2}^{(2)} \\ Z_{C_2}^{(2)} \end{bmatrix}$ $\left[D_2^{(2)}\right] = \begin{bmatrix} X_{D_2}^{(2)} \\ Y_{D_2}^{(2)} \\ Z_{D_2}^{(2)} \end{bmatrix}, \left[P_2^{(2)}\right] = \begin{bmatrix} X_{P_2}^{(2)} \\ Y_{P_2}^{(2)} \\ Z_{P_2}^{(2)} \end{bmatrix}, \left[Q_2^{(2)}\right] = \begin{bmatrix} X_{Q_2}^{(2)} \\ Y_{Q_2}^{(2)} \\ Z_{Q_2}^{(2)} \end{bmatrix}$

The indirect connections AA_2, BB_2, CC_2 and $DD_2$are geometrically defined through the constant lengths between the respective joints L_{AA2}, L_{BB2}, L_{CC2} and L_{DD2}.

4. The position and orientation of the mobile platform

The position and orientation of the platform 2 is described by 6 generalized coordinates: the coordinates of the origin O_2 of the mobile system $O_2X_2Y_2Z_2$(of the mobile platform 2) relative to the fixed system OXYZ and the Bryant angles ϕ_1, ϕ_2, and ϕ_3 described in figure 4.

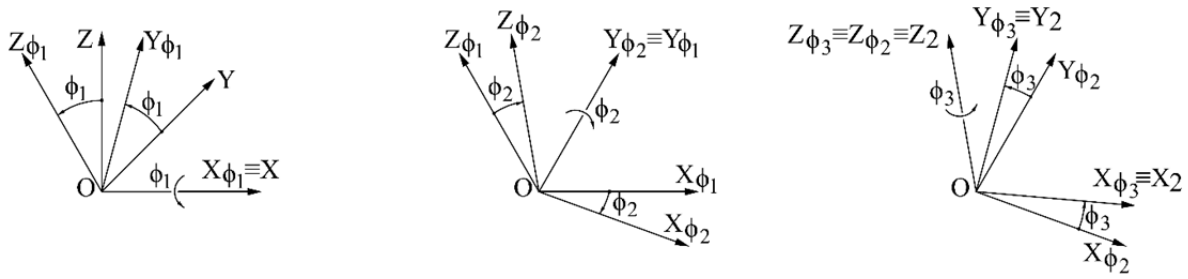

Figure 4. Bryant angles ϕ_1, ϕ_2, and ϕ_3 describing the orientation of the mobile system $O_2X_2Y_2Z_2$ of the mobile platform 2 relative to the fixed system OXYZ.

The corresponding rotation matrix are:

$$\left[M_{\phi_1}\right]=\begin{bmatrix}1 & 0 & 0\\ 0 & \cos\phi_1 & -\sin\phi_1\\ 0 & \sin\phi_1 & \cos\phi_1\end{bmatrix},\left[M_{\phi_2}\right]=\begin{bmatrix}\cos\phi_2 & 0 & \sin\phi_2\\ 0 & 1 & 0\\ -\sin\phi_2 & 0 & \cos\phi_2\end{bmatrix},\left[M_{\phi_3}\right]=\begin{bmatrix}\cos\phi_3 & -\sin\phi_3 & 0\\ \sin\phi_3 & \cos\phi_3 & 0\\ 0 & 0 & 1\end{bmatrix} \quad (2)$$

and the general rotation matrix is:

$$[M_2]=\left[M_{\phi_1}\right]\left[M_{\phi_2}\right]\left[M_{\phi_3}\right]=$$

$$\begin{bmatrix}\cos\phi_2\cos\phi_3 & -\cos\phi_2\sin\phi_3 & \sin\phi_2\\ \cos\phi_1\sin\phi_3+\sin\phi_1\sin\phi_2\cos\phi_3 & \cos\phi_1\cos\phi_3-\sin\phi_1\sin\phi_2\sin\phi_3 & -\sin\phi_1\cos\phi_2\\ \sin\phi_1\sin\phi_3-\cos\phi_1\sin\phi_2\cos\phi_3 & \sin\phi_1\cos\phi_3+\cos\phi_1\sin\phi_2\sin\phi_3 & \cos\phi_1\cos\phi_2\end{bmatrix} \quad (3)$$

The elevation α_n and azimuthal ψ_n angles (eigure 5) are calculated with equation(4).

$$\alpha_n=90°-\theta_n=90-\cos^{-1}(n_z);\ \psi_n=\tan^{-1}\frac{n_x}{n_y} \quad (4)$$

wheren_x, n_y, n_z are the direction cosines of O_2Z_2 axis in OXYZ system (the last column in matrix 3).

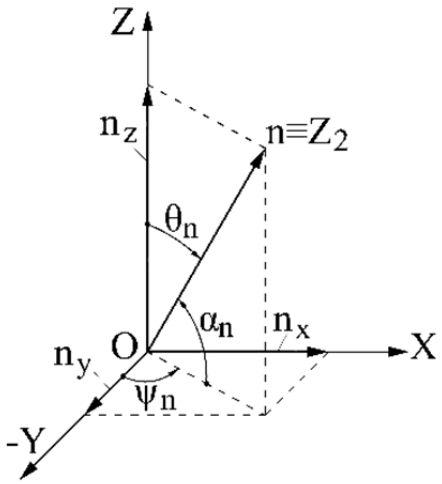

Figure 5. Elevation and azimuthal angles of the mobile platform.

5. The position functions

The system of the position functions (equation 5) consists of fourequations describing the geometrical constraints (equationF1 to F4) and two driving constraints equations (equationF5 and F6). Thus, the system has 6 equations and 6 unknowns: X_{O2}, Y_{O2}, Z_{O2}, ϕ_1, ϕ_2, ϕ_3.

The general form of the equations is:

$$\begin{aligned}
&F_1{:}(X_A - X_{A2})^2 + (Y_A - Y_{A2})^2 + (Z_A - Z_{A2})^2 - L_{AA_2}^2 = 0\\
&F_2{:}(X_B - X_{B2})^2 + (Y_B - Y_{B2})^2 + (Z_B - Z_{B2})^2 - L_{BB_2}^2 = 0\\
&F_3{:}(X_C - X_{C2})^2 + (Y_C - Y_{C2})^2 + (Z_C - Z_{C2})^2 - L_{CC_2}^2 = 0\\
&F_4{:}(X_D - X_{D2})^2 + (Y_D - Y_{D2})^2 + (Z_D - Z_{D2})^2 - L_{DD_2}^2 = 0\\
&F_5{:}(X_P - X_{P2})^2 + (Y_P - Y_{P2})^2 + (Z_P - Z_{P2})^2 - L_{PP_2}^2 = 0\\
&F_6{:}(X_Q - X_{Q2})^2 + (Y_Q - Y_{Q2})^2 + (Z_Q - Z_{Q2})^2 - L_{QQ_2}^2 = 0
\end{aligned} \tag{5}$$

The system described by (5) is nonlinear and can be solved by numerical methods, usually by Newton-Raphson algorithm. The mechanism configuration for which the mobile platform 2 is parallel with the fixed platform 1 is considered as initial solution.

In this case,

$$\left(X_{O_2}\right)_0 = 0, \left(Y_{O_2}\right)_0 = 0, \left(Z_{O_2}\right)_0 = OO_2, (\phi_1)_0 = 0, (\phi_2)_0 = 0, (\phi_3)_0 = 0, \tag{6}$$

$$\left(L_{PP_2}\right)_0 = \sqrt{\left(X_P - X_{P_2}\right)^2 + \left(Y_P - Y_{P_2}\right)^2 + \left(Z_P - Z_{P_2}\right)^2} \tag{7}$$

$$\left(L_{QQ_2}\right)_0 = \sqrt{\left(X_Q - X_{Q_2}\right)^2 + \left(Y_Q - Y_{Q_2}\right)^2 + \left(Z_Q - Z_{Q_2}\right)^2} \tag{8}$$

$$X_{P_2} = X_{P_2}^{(2)},\ Y_{P_2} = Y_{P_2}^{(2)}, Z_{P_2} = OO_2 + Z_{P_2}^{(2)}, X_{Q_2} = X_{Q_2}^{(2)},\ Y_{Q_2} = Y_{Q_2}^{(2)}, Z_{Q_2} = OO_2 + Z_{Q_2}^{(2)} \tag{9}$$

The coordinates of the points A_2, B_2, C_2 and D_2in the system (5) are given by:

$$\begin{bmatrix} X_{A_2} \\ Y_{A_2} \\ Z_{A_2} \end{bmatrix} = \begin{bmatrix} X_{O_2} \\ Y_{O_2} \\ Z_{O_2} \end{bmatrix} + [M_2] \begin{bmatrix} X_{A_2}^{(2)} \\ Y_{A_2}^{(2)} \\ Z_{A_2}^{(2)} \end{bmatrix}, \quad \begin{bmatrix} X_{B_2} \\ Y_{B_2} \\ Z_{B_2} \end{bmatrix} = \begin{bmatrix} X_{O_2} \\ Y_{O_2} \\ Z_{O_2} \end{bmatrix} + [M_2] \begin{bmatrix} X_{B_2}^{(2)} \\ Y_{B_2}^{(2)} \\ Z_{B_2}^{(2)} \end{bmatrix} \tag{10}$$

$$\begin{bmatrix} X_{C_2} \\ Y_{C_2} \\ Z_{C_2} \end{bmatrix} = \begin{bmatrix} X_{O_2} \\ Y_{O_2} \\ Z_{O_2} \end{bmatrix} + [M_2] \begin{bmatrix} X_{C_2}^{(2)} \\ Y_{C_2}^{(2)} \\ Z_{C_2}^{(2)} \end{bmatrix}, \quad \begin{bmatrix} X_{D_2} \\ Y_{D_2} \\ Z_{D_2} \end{bmatrix} = \begin{bmatrix} X_{O_2} \\ Y_{O_2} \\ Z_{O_2} \end{bmatrix} + [M_2] \begin{bmatrix} X_{D_2}^{(2)} \\ Y_{D_2}^{(2)} \\ Z_{D_2}^{(2)} \end{bmatrix}$$

Thus, the system (5) has the general form

$$\left[F_i\left(X_{O_2}, Y_{O_2}, Z_{O_2},\ \phi_1, \phi_2, \phi_3, \mathrm{t}\right)\right] = 0 \tag{11}$$

where:time t is under explicit form in the equations corresponding to the driving constraints:

$$L_{PP_2} = L_{PP_2 min} + a_1 \cdot t_1, \quad L_{QQ_2} = L_{QQ_2 min} + a_2 \cdot t_2 \tag{12}$$

and $a_{1,2}$are the linear actuators velocities in mm/s.

For the initial configuration:

$$(t_1)_0 = \frac{\left(L_{PP_2}\right)_0 - L_{PP_2 min}}{a_1},\ (t_2)_0 = \frac{\left(L_{QQ}\right)_0 - L_{QQ_2 min}}{a_2} \tag{13}$$

For the next configurations:

$$t_1 = (t_1)_0 \pm \Delta t_1,\ t_2 = (t_2)_0 \pm \Delta t_2 \tag{14}$$

considering"+" for increasing L_{PP_2}, L_{QQ_2} and "-" for decreasing L_{PP_2}, L_{QQ_2}.

The incident angle defined as the angle between the sunray direction (figure 1) and the normal to the mobile platform (direction O_2Z_2) is required to assess the tracking efficiency. This angle is given by:

$$\nu = \cos^{-1}(cos\,\alpha \cdot cos\,\alpha_n \cdot cos(\psi - \psi_n) + sin\,\alpha \cdot sin\,\alpha_n) \tag{15}$$

where α_n and ψ_n are the elevation and diurnal angles of the mobile platform 2.

6. The velocity functions

To evaluate the pressure angle, the velocities of the points P_2 and Q_2 are required. These are given by:

$$\begin{bmatrix}\dot{X}_{P_2}\\ \dot{Y}_{P_2}\\ \dot{Z}_{P_2}\end{bmatrix} = \begin{bmatrix}\dot{X}_{O_2}\\ \dot{Y}_{O_2}\\ \dot{Z}_{O_2}\end{bmatrix} + [\dot{M}_2]\begin{bmatrix}X^{(2)}_{P_2}\\ X^{(2)}_{P_2}\\ X^{(2)}_{P_2}\end{bmatrix}, \qquad \begin{bmatrix}\dot{X}_{Q_2}\\ \dot{Y}_{Q_2}\\ \dot{Z}_{Q_2}\end{bmatrix} = \begin{bmatrix}\dot{X}_{O_2}\\ \dot{Y}_{O_2}\\ \dot{Z}_{O_2}\end{bmatrix} + [\dot{M}_2]\begin{bmatrix}X^{(2)}_{Q_2}\\ X^{(2)}_{Q_2}\\ X^{(2)}_{Q_2}\end{bmatrix} \tag{16}$$

where the generalized velocities:

$$[\dot{q}]=\left[\dot{X}_{O_2}\dot{Y}_{O_2}\dot{Z}_{O_2}\dot{\phi}_1\dot{\phi}_2\dot{\phi}_3\right]^T \tag{17}$$

can be obtained from the first derivative of the equations in system (4) relative to time, which leads to the general form:

$$[J][\dot{q}] = -\left[\frac{\partial F}{\partial t}\right] \tag{18}$$

where [J] is the Jacobian of the system (4), and $\left[\frac{\partial F}{\partial t}\right]$ has the form as given by (19):

$$\left[\frac{\partial F}{\partial t}\right] = \left[0\ \ 0\ \ 0\ \ 0\ \ -2a_1L_{PP_2}\ \ -2a_2L_{QQ_2}\right]^T \tag{19}$$

In (16), $[\dot{M}_2]$is given by:

$$[\dot{M}_2] = \frac{\partial[M_2]}{\partial\phi_1}\dot{\phi}_1 + \frac{\partial[M_2]}{\partial\phi_2}\dot{\phi}_2 + \frac{\partial[M_2]}{\partial\phi_3}\dot{\phi}_3 \tag{20}$$

7. The pressure angles

The pressure angles (β_P and β_Q) can be obtained from the scalar product of the actuators direction and absolute velocity vectors of the points of interest P_2 and Q_2

$$\beta_P = \cos^{-1}\left(\frac{\overrightarrow{PP_2}\cdot\overrightarrow{v_{P_2}}}{|PP_2|\cdot|v_{P_2}|}\right) \tag{21}$$

where:

$$\overrightarrow{PP_2} = \left(X_P - X_{P_2}\right)\mathrm{i} + \left(Y_P - Y_{P_2}\right)\mathrm{j} + \left(Z_P - Z_{P_2}\right)\mathrm{k} \tag{22}$$

$$\overrightarrow{v_{P_2}} = \dot{X}_{P_2}\mathrm{i} + \dot{Y}_{P_2}\mathrm{j} + \dot{Z}_{P_2}\mathrm{k} \tag{23}$$

$$|PP_2| = \sqrt{\left(X_P - X_{P_2}\right)^2 + \left(Y_P - Y_{P_2}\right)^2 + \left(Z_P - Z_{P_2}\right)^2} \tag{24}$$

$$\left|v_{P_2}\right| = \sqrt{\dot{X}_{P_2}{}^2 + \dot{Y}_{P_2}{}^2 + \dot{Z}_{P_2}{}^2} \tag{25}$$

8. Numerical example

This parallel tracking mechanism was virtually prototyped in SolidWorks, and two motion studies are further presented, for the mechanism positioning the mobile platform from the initial configuration (figure 6a – horizontal position) towards East (figure 6b) and, respectively towardsWest (figure 6c).

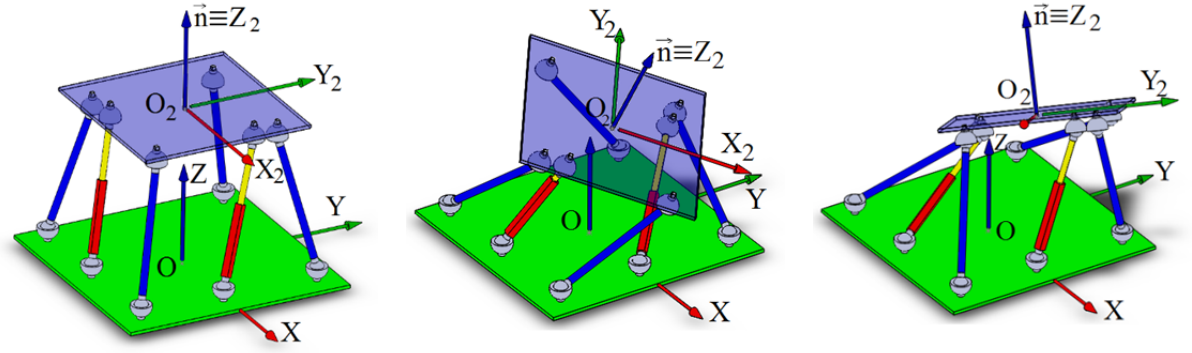

Figure 6. Parallel tracking mechanism positions: initial (a), East (b) and West (c).

The geometrical model of the proposed parallel tracking mechanism is presented in table 3.

Table 3. Geometrical model of the bodies.

Body	**Cartesian coordinates**
Body 1	$[A]=\begin{bmatrix}X_A\\Y_A\\Z_A\end{bmatrix}=\begin{bmatrix}-800\\-800\\150\end{bmatrix}$, $[B]=\begin{bmatrix}X_B\\Y_B\\Z_B\end{bmatrix}=\begin{bmatrix}-800\\800\\150\end{bmatrix}$, $[C]=\begin{bmatrix}X_C\\Y_C\\Z_C\end{bmatrix}=\begin{bmatrix}800\\800\\150\end{bmatrix}$ $[D]=\begin{bmatrix}X_D\\Y_D\\Z_D\end{bmatrix}=\begin{bmatrix}800\\-800\\150\end{bmatrix}$, $[P]=\begin{bmatrix}X_P\\Y_P\\Z_P\end{bmatrix}=\begin{bmatrix}0\\-800\\150\end{bmatrix}$, $Q=\begin{bmatrix}X_Q\\Y_Q\\Z_Q\end{bmatrix}=\begin{bmatrix}800\\0\\150\end{bmatrix}$
Body 2	$\left[A_2^{(2)}\right]=\begin{bmatrix}X_{A_2}^{(2)}\\Y_{A_2}^{(2)}\\Z_{A_2}^{(2)}\end{bmatrix}=\begin{bmatrix}-550\\-550\\-150\end{bmatrix}$, $\left[B_2^{(2)}\right]=\begin{bmatrix}X_{B_2}^{(2)}\\Y_{B_2}^{(2)}\\Z_{B_2}^{(2)}\end{bmatrix}=\begin{bmatrix}-550\\550\\-150\end{bmatrix}$, $\left[C_2^{(2)}\right]=\begin{bmatrix}X_{C_2}^{(2)}\\Y_{C_2}^{(2)}\\Z_{C_2}^{(2)}\end{bmatrix}=\begin{bmatrix}550\\550\\-150\end{bmatrix}$ $\left[D_2^{(2)}\right]=\begin{bmatrix}X_{D_2}^{(2)}\\Y_{D_2}^{(2)}\\Z_{D_2}^{(2)}\end{bmatrix}=\begin{bmatrix}550\\-550\\-150\end{bmatrix}$, $\left[P_2^{(2)}\right]=\begin{bmatrix}X_{P_2}^{(2)}\\Y_{P_2}^{(2)}\\Z_{P_2}^{(2)}\end{bmatrix}=\begin{bmatrix}-335\\-550\\-150\end{bmatrix}$, $\left[Q_2^{(2)}\right]=\begin{bmatrix}X_{Q_2}^{(2)}\\Y_{Q_2}^{(2)}\\Z_{Q_2}^{(2)}\end{bmatrix}=\begin{bmatrix}550\\335\\-150\end{bmatrix}$

The positionsof the mobile platform 2 during the motion fromhorizontal towards theEast and West positionsare defined through the coordinates of its reference system origin O_2 and Bryant angles presented in table 4 and 5, respectively along with its elevation and azimuth. As driving motions are considered the linear actuator velocities a_1=75mm/s and a_2=15mm/s.

Table 4. Positions of the mobile platform during its motion from horizontal to East position.

Time	**Platform origin coordinates**			**Bryant angles**			**Elevation**	**Azimuth**
t [s]	X_{O2} **[mm]**	Y_{O2} **[mm]**	Z_{O2} **[mm]**	ϕ_1 **[°]**	ϕ_2 **[°]**	ϕ_3 **[°]**	α_n **[°]**	ψ_n **[°]**
0	0.00	0.00	1375.74	0.00	0.00	0.00	90.00	90.00
1	54.48	20.72	1357.25	0.69	11.77	1.80	88.22	83.92
2	28.14	28.82	1293.97	0.98	25.76	2.12	88.05	78.38
3	-4.11	-20.49	1195.79	0.25	37.96	-0.72	89.40	71.81
4	-26.11	-113.35	1060.28	-4.47	48.03	-11.13	81.87	65.95
5	-31.26	-235.13	869.58	-18.17	52.32	-37.01	65.37	62.00

Table 5. Positions of the mobile platform during its motion from horizontal to West position.

Time	**Platform origin coordinates**			**Bryant angles**			**Elevation**	**Azimuth**
t [s]	X_{O2} **[mm]**	Y_{O2} **[mm]**	Z_{O2} **[mm]**	ϕ_1 **[°]**	ϕ_2 **[°]**	ϕ_3 **[°]**	α_n **[°]**	ψ_n **[°]**
0	0.00	0.00	1375.74	0.00	0.00	0.00	90.00	-90.00
1	200.28	49.94	1347.77	0.79	6.14	5.49	84.53	-86.54
2	171.33	164.81	1295.53	2.04	19.29	9.06	81.33	-80.49
3	135.05	226.77	1214.55	4.39	29.64	14.62	76.87	-75.08
4	102.42	257.43	1119.34	7.94	37.75	21.54	72.07	-70.60
5	73.90	269.93	1013.83	12.81	44.00	29.90	67.05	-66.85

Based on the coordinates of the linear actuators joints (P_2 and Q_2)the lengths of the linear actuators during the motion from horizontal to East position are presented in table 6.

Table 6. Linear actuators joints coordinateson the mobile platform, and linear actuators lengths variation during the motion from horizontal to the East position.

Time	**Linear actuators joints coordinates [mm]**						**Linear actuators lengths [mm]**	
t [s]	X_{P_2}	Y_{P_2}	Z_{P_2}	X_{Q_2}	Y_{Q_2}	Z_{Q_2}	L_{PP2}	L_{QQ2}
0	-313.6	-512.2	1185.8	521.8	345.1	1180.9	1019.4	1056.8
1	-158.5	-596.8	1155.7	496.0	403.3	1177.9	944.4	1081.8
2	-52.2	-639.8	1093.1	356.5	477.6	1119.5	869.4	1106.8
3	30.1	-601.2	1005.3	208.0	568.9	1012.6	794.4	1131.8
4	95.5	-508.3	888.4	69.1	668.8	851.4	719.4	1156.8
5	137.5	-391.6	728.7	-56.0	761.5	618.1	644.4	1181.8

Based on the position and velocity vectors of the points of interest P_2 and Q_2, the pressure angles in these joints are evaluated and the values are presented in table 7

Table 7. Velocity and pressure angles of the joints $P_2$and Q_2during the motion from horizontal to the East position.

Time	**Velocities of the joints P_2 and Q_2 [mm/s]**								**Pressure angles [°]**	
t [s]	$\dot{X}_{P_2}$	$\dot{Y}_{P_2}$	$\dot{Z}_{P_2}$	v_{P_2}	$\dot{X}_{Q_2}$	$\dot{Y}_{Q_2}$	$\dot{Z}_{Q_2}$	v_{Q_2}	β_{P_2}	β_{Q_2}
0	185.0	-41.7	-21.7	190.8	80.4	80.4	26.2	116.7	66.9	74.1
1	125.4	-88.1	-45.7	159.9	-112.7	-112.7	-32.3	162.6	62.1	74.7
2	91.9	2.2	-76.2	119.4	-150.2	-150.2	-82.8	228.0	51.1	70.0
3	73.7	70.1	-100.3	142.9	-144.7	-144.7	-132.0	243.5	58.3	66.5
4	56.1	111.2	-136.4	184.7	-132.6	-132.6	-193.7	269.5	66.0	66.1
5	22.9	112.4	-180.7	214.1	-117.1	-117.1	-275.3	321.3	69.5	72.0

The results for the elevation angle (α_n), azimuthal angle (ψ_n) and pressure angle (β_{P2}, β_{Q2}) depend on the mechanism geometry, driving actuators position and velocity. Numerical results validate the linkage analytical model. An optimum design based on these parameters is required in the next step to allow the necessary positions of the mobile platform with acceptable pressure angles.

9. Conclusions

A new mechanism, of parallel linkage type, is proposed to track solar thermal platforms installed on ships. The mechanism has four connections SS type between the mobile platform and the basis and two driving linear actuators connected to the basis and mobile platform (two absolute motions). This mechanism allows to get the necessary position of the mobile platform according to the specific motions of the ships on different latitudes. The paper describes the analytical model and validates it through a numerical example. As a next step, the mechanism synthesis is necessary to get the optimal collection efficiency of the available solar radiation (defined by the incident angle between the Sunray and the normal to the mobile platform) and the optimum mechanism functionality (pressure angles and actuator strokes, relative motions in the spherical joints, loads).

10. References

[1] Visa I, Jaliu C, Duta A, Neagoe M, Comsit M, Moldovan M, Ciobanu D, Burduhos B, Saulescu R 2015 *The role of mechanisms in sustainable Energy Systems* (Transilvania University Publishing House)

[2] Neagoe M, Visa I, Burduhos B G, Moldovan M D 2014 Thermal Load based Adaptive Tracking for Flat Plate Solar Collectors *Energy Procedia* **48** pp 72-78

[3] Moldovan M, Visa I, Saulescu R, Comsit M 2014 Four-bar linkages with linear actuators used for solar trackers with large angular diurnal strokes *The 11th IFToMM International Symposium on Science of Mechanisms and Machines, Mechanisms and Machine Science* **18** pp 411-423

[4] Alizade R I, Can F C, Gezgin E, Selvi O 2007 Structural Synthesis of New Parallel and Serial Platform Manipulators *Proceedings of the 12th IFToMM World Congress, Besançon France*

[5] Quaglia G and Maurino S L 2016 Solar.q_1: A new solar-tracking mechanism based on four-bar linkages *Journal of Mechanical Engineering Science* pp 1–13

[6] Visa I, Neagoe M, Moldovan M and Comsit M 2014 Synthesis of Parallel Linkages by Multibody Systems Method *Applied Mechanics and Materials* **658** pp 153-158

[7] Carrasco Martinez C M 2008 Bidirectional solar tracker *Patent no CA 2673989 A1*

[8] Oosting K 2010 Actuated feedforward controlled solar tracking systems *Patent no US*

2010/0180883 A1

[9] Haug J E 1989 *Computer aided kinematics and dynamics of mechanical systems, Vol. I: Basic Methods* (USA: Allyn and Bacon)

Acknowledgments

We hereby acknowledge the structural founds project PRO-DD (POS-CCE, O.2.2.1., ID 123, SMIS 2637, contract no. 11/2009) for providing the infrastructure used in this work and the project PNII Cooperation Project, EST in URBA no. 28/2012 financially supported by the Romanian National Research Council.